



Published in final edited form as:

*Radiology*. 2007 December ; 245(3): 824–830. doi:10.1148/radiol.2453061889.

## Blood Vessel Morphological Changes as Visualized by MRA During Treatment of Brain Metastases: A Feasibility Study

Elizabeth Bullitt, MD<sup>1</sup>, Nancy U. Lin, MD<sup>2</sup>, J. Keith Smith, MD, PhD<sup>1</sup>, Donglin Zeng, PhD<sup>1</sup>, Eric P. Winer, MD<sup>2</sup>, Lisa A. Carey, MD<sup>1</sup>, Weili Lin, PhD<sup>1</sup>, and Matthew G. Ewend, MD<sup>1</sup>

<sup>1</sup> CASILab, CB # 7062, University of North Carolina, Chapel Hill, NC 27599, USA

<sup>2</sup> Dana-Farber/Harvard Cancer Center, Boston, MA 02115, USA

### Abstract

**Purpose**—To prospectively determine a) if magnetic resonance angiograms (MRA) can detect intracranial vascular morphological changes during treatment of brain metastases from breast cancer, and b) if serial, quantitative vessel tortuosity measurements might predict tumor treatment response in advance of traditional methods.

**Materials and Methods**—Institutional review board approval and informed consent were obtained in this HIPAA-compliant study. Twenty-two women aged 31–61 underwent brain MRA imaging prior to and two months after initiation of lapatinib therapy for brain metastases from breast cancer. Vessels were extracted from MRA using a computer program. Changes in vessel number, radius, and tortuosity were calculated mathematically, were normalized by values defined from 34 healthy controls (19 females, 15 males, age range 19–72), and were compared to subsequent assessments of tumor volume and clinical course.

**Results**—All tumor patients exhibited abnormal vessel tortuosity at baseline. Nineteen patients (86%) failed to exhibit improvement in vessel tortuosity at month 2 and all demonstrated tumor growth by month 4. Vessel tortuosity measurements correctly predicted treatment failure 1–2 months earlier than traditional methods. Three patients (14%) displayed quantitative improvement in vessel tortuosity at month 2, with dropout of small abnormal vessels and “straightening” of large vessels. The two patients for whom further follow-up was available each responded to treatment for over 6 months.

**Conclusion**—Our results establish the feasibility of using MRA to quantify vessel shape changes during therapy. Although further research is required, results suggest that changes in vessel tortuosity might provide an early prediction of tumor treatment response.

### Keywords

cancer; breast; brain; vessel; MRA; tortuosity

### Advances in Knowledge

1. Noninvasive magnetic resonance angiography (MRA) can depict vascular morphological changes during treatment of brain metastases in human patients.

Contact information: Elizabeth Bullitt MD, CASILab, 349 Wing C, CB #7062, University of North Carolina, Chapel Hill, NC, 27599, (919) 843-3101, Fax: (919) 843-1500, bullitt@med.unc.edu.

Clinical trial registration #: NCT00098605, <http://clinicaltrials.gov/>

2. A computer-assisted approach permits both quantitative measurement of vessel shape and visualization of vessel shape changes during treatment.
3. Normalization or lack of normalization of abnormal, tumor-induced vessel tortuosity may predict tumor treatment response.
4. Individual vessels can be followed over time, enabling perception of complex vascular alterations.

## Implications for Patient Care

Changes in vessel morphology, as computed from non-invasively acquired magnetic resonance angiograms, may provide an early indicator of brain tumor response to chemotherapy. This ability has the potential to allow early, responsive adjustment of treatment tailored to the individual patient.

## INTRODUCTION

Angiogenesis, the outgrowth of new blood vessels from existing vessels, is necessary for tumor growth beyond 1–2 mm<sup>3</sup> (1). One investigational impediment is the lack of a noninvasive imaging method that can monitor individual vessels over time (2).

Vessel tortuosity is of particular interest. Within 24 hours of injection of 20–50 cancer cells in animal models, initially healthy vessels in the tumor vicinity become abnormally tortuous (3). This abnormality extends beyond tumor boundaries and precedes vascular sprouting (3). Baish aptly describes the typical abnormal configuration as “many smaller bends upon each larger bend” (4). Abnormal vascular tortuosity is associated not only with malignancy in animal models but also with a range of cancers in human patients (5–7). The etiology may be related to growth-factor-related changes to the vessel wall, including alteration of the basement membrane, loss of pericytes and smooth muscle, and proliferation of endothelial cells (8). In animals, cancer-associated vessel tortuosity abnormalities are known to resolve during anti-angiogenic treatment (3,9–10).

The purpose of this study was to prospectively determine a) if magnetic resonance angiograms (MRA) can detect intracranial vascular morphological changes during treatment of brain metastases from breast cancer even if current MRA imaging technology cannot perceive capillaries, and b) if serial, quantitative vessel tortuosity measurements can predict tumor treatment response in advance of traditional methods.

## MATERIALS AND METHODS

### Patient Groups

Our study evaluated the images of a subset of tumor patients enrolled in an underlying drug trial and the images of healthy controls. All three studies (the underlying drug trial, our tumor imaging study, and the collection of healthy control images) were HIPAA compliant, IRB approved, and required signed informed consent.

Tumor patients involved in our imaging study comprised 22 of a total of 39 women enrolled in a multi-center, Phase II trial of lapatinib (GW572106, GlaxoSmithKline) in the treatment of HER-2 positive breast cancer metastatic to brain. Eligibility for enrollment in the drug study included HER2+ breast cancer, new or progressive brain metastases, and at least one lesion of diameter 1 cm or more. The underlying drug study was presented at a conference (11) and will be reported independently. Our imaging study included all 22 patients (female, age range 31–61, mean age 52 years) who consented to enter the imaging study and for whom an MRA was

acquired both at baseline and at month two. An interim report on the imaging study was presented at a computer science conference (12).

An MRA image database of 34 healthy controls without history of hypertension, diabetes, cancer, and neurological or psychiatric disease established the basis of “healthy”. Subjects ranged in age from 19–72 (mean age 38) and included 19 females and 15 males. This database was used to derive means and standard deviations of healthy vessel shape parameters without age or sex matching to individual tumor patients.

### Image Acquisition and Clinical Study Endpoint

The underlying clinical trial acquired T1, T2, and T1-gadolinium enhanced images at baseline, at month 2, and every two months thereafter until the patient was withdrawn from study (criteria for withdrawal are given below). Our secondary imaging study additionally obtained MRA images at baseline and at month 2.

Different institutions employed MR units made by different vendors. All institutions were required to obtain MRA images using a standardized format and to perform sequential MRAs of the same patient upon the same machine. MRA images were acquired as 3D-time-of-flight prior to gadolinium injection, covered the entire head using multiple (5) overlapping (25%) thin slabs (MOTSA), and employed a magnetization transfer pulse for background suppression of white matter. Voxel size was  $0.5 \times 0.5 \times 0.8 \text{ mm}^3$ . TR/TE/flip\_angle/were respectively 35msec/3msec/22. Although the base matrix was 448x448, a rectangular FOV of 0.786 and partial Fourier of 0.8 were employed to reduce data acquisition time to 18 minutes.

Patients were treated under the underlying drug trial until progression of disease, toxicity, or withdrawal of consent. Progressive brain disease was defined from gadolinium enhanced MR as greater than a 20% increase in the sum of longest dimensions of target lesions, an increase of at least 5 mm in the longest dimension of at least one lesion, and/or the appearance of one or more new lesions greater than or equal to 6 mm (“Response Evaluation Criteria in Solid Tumors”; RECIST (13)). Judgment of progressive disease was made by the treating physician with the assistance of clinical radiologists. Six site physicians were involved with, collectively, over 90 years experience in treating breast cancer (coauthors NUL, JKS, EPW, LAC, and MGE were involved clinicians). No patients now remain in the study as a result of progressive disease or death.

### Image Processing: Vessels

For our imaging study, digital images of tumor patients were sent for processing to an individual uninvolved in patient care (EB). Findings of our research study were not used clinically, as was understood by the tumor patients involved. EB was blinded to each patient’s clinical status until image analysis was completed and had been reported to the central clinical group.

Image processing was performed by computer programs applied by EB. Vessels were segmented from the entire brain (14) and post-processed to provide a connected set of vessel trees (15). Each vessel was mathematically described as an ordered list of 4-dimensional vector values, in which the first three values represented an x,y,z spatial point along the vessel skeleton and the fourth the associated radius (14,15). This method defines tubular objects of higher intensity than background (14,15) and thus was not impeded by MOTSA’s “Venetian blind” effect. It took approximately thirty minutes to extract vessel trees for each subject.

Although the program can calculate shape measures for vessels clipped to the region of an individual tumor (7), many patients in the current study had numerous metastases. It was not feasible to analyze many regions of interest. Each patient’s segmented vasculature was therefore analyzed as a whole, with results for each parameter averaged over the brain.

Shape measures were calculated automatically. Measurements included

- **Vessel number:** the number of individual, unbranched vessels. Results were reported as integers.
- **Average radius:** the sum of radii at all vessel skeleton points divided by the number of points. Results were reported in mm.
- **Average vessel tortuosity by the Sum of Angles Metric (SOAM):** SOAM sums curvature along a space curve using successive trios of equally spaced vessel skeleton points and normalizes by vessel length (16). SOAM values are elevated in the presence of high-frequency, low-amplitude bends. Values were reported as radians/cm.
- **Average vessel tortuosity by the Inflection Count Metric (ICM):** The ICM calculates the number of “inflection” points along a space curve and multiplies this number (plus 1) by the total path length of the curve divided by the distance between endpoints (16). ICM values are elevated when a curve exhibits a high amplitude sinusoidal pattern. Values were reported as a dimensionless number.
- **Malignancy Probability (MP):** The MP equation was derived from a study of multiple vessel shape parameters in patients with a variety of tumor types (7). In that study, discriminant analysis indicated that only a weighted combination of the SOAM and ICM tortuosity measures appeared effective in separating benign from malignant disease. To calculate MP, the SOAM and ICM measures are first normalized (z-scored) by the means and standard deviations of healthy values over the same region of interest and are then combined:

$$X = 1.7160 * z - \text{scoredSOAM} + 0.51241 * z - \text{scoredICM} - 2.8659$$

$$Y = -0.24876 * z - \text{scoredSOAM} - 0.58972 * z - \text{scoredICM} - 0.19672$$

The probability/possibility of malignancy was then

$$\frac{\exp(X)}{\exp(X) + \exp(Y)}$$

The calculated probability/possibility of malignancy for each tumor test case will range from 0 to 1 (equivalently from 0% to 100%). Higher values indicate a higher probability/possibility of malignancy. In essence, this equation provides a quantitative formulation of Baish’s phrase “Many smaller bends upon each larger bend” (4), with SOAM sensitive to small bends and ICM to larger bends (7).

### Image Processing: Tumors

A difficulty with the unidimensional RECIST measurements used in the underlying clinical trial is that sequential estimates of tumor size may be confounded by change in imaging slice angle. As part of the research protocol, tumor volumes were therefore calculated from gadolinium-enhanced T1 images for all lesions 1 cm<sup>3</sup> or more using a program that defined tumors via polygon drawing and filling on orthogonal cuts through an image volume. EB selected the tumors for analysis. Tumor volume was automatically calculated as the number of labeled voxels multiplied by voxel size, with results expressed in cm<sup>3</sup>. A meaningful increase (decrease) in tumor volume was predefined as a volumetric increase (decrease) from baseline of at least 20% with a concomitant change in volume of at least 0.5 cm<sup>3</sup>. Treatment failure based on volumetrics was predefined as growth by 20% and 0.5 cm<sup>3</sup> of either a single lesion or the sum of all segmented lesions.

**Data Analyses**—The means and standard deviations of vessel number, average radius, SOAM, and ICM were calculated for healthy controls, for the tumor group at baseline and at month 2, and for the subsets of tumor patients who did and did not exhibit improvement in MP at month 2. The means and standard deviations of MP were also calculated for tumor patients at both time points.

We compared change in MP at month 2 both to the patient's subsequent clinical course and to subsequent tumor volumetric calculations. A drop in MP of 20 was predefined as indicative of vascular normalization. For patients who failed to exhibit improvement in MP at month 2, the means and standard deviations of the time to treatment failure were calculated both for clinical and for volumetric criteria. For the 3 patients whose MP decreased at month 2, we provide clinical and volumetric information for each patient individually.

An interesting question was whether normalization of vessel tortuosity was related to dropout of small, abnormal vessels, to “straightening” of initially tortuous vessels, or both. It was also of interest to determine if vessels exhibiting “straightening” could lie outside tumor boundaries. We therefore examined segmented vessels and tumors using a 3D display and manually sought four examples of major named vessels that could be identified from one scan to the next, whose appearance changed over time, and that lay totally or partially outside of tumor confines. Selected vessels included a pair of frontopolar arteries in one patient and a posterior cerebral and a superior cerebellar artery in a second patient. The display interface offered the option of clicking on an individual vessel and “hiding” it and its associated subtree; we did so in some illustrations to prevent obscuration of vessels of interest by a plethora of tiny branches; the original quantitative analysis involved the entire intracerebral vasculature. Finally, the display interface offered the option of clicking on an individual vessel with subsequent report of that vessel's morphology. We thereby examined change in radius of the four major named vessels manually selected as examples of vascular normalization.

## RESULTS

All tumor patients exhibited marked vessel tortuosity abnormalities at baseline (Table 1). Nineteen patients exhibited no improvement in MP at month 2. Nine of these showed marked increase in tumor size by both RECIST (13) and volumetric criteria at month 2 and were immediately withdrawn from study. The remaining ten exhibited stability or decrease in tumor volume at month 2, suggesting at least transient drug response. However, all of these potentially responsive patients demonstrated tumor growth volumetrically on T1 images at month 4 and, when later images were available, steady tumor growth thereafter. The number of months required to recognize treatment failure was 3.9 + 1.6 months by clinical criteria, 3.1 + 1.4 months by volumetric measurement, and 2 + 0 months by vessel shape analysis.

### Reduction in MP

Three patients exhibited reduction in MP at month 2. Patient R1 (Figure 1) possessed a single large tumor. Her MP dropped from 100% to 64% at month 2, concomitant with a reduction in tumor volume of 61% (18.4 to 7.2 cm<sup>3</sup>). Her tumor continued to regress, exhibiting an 85% (to 2.7 cm<sup>3</sup>) volume reduction at month 4 with stability thereafter. This patient exhibited the longest clinical remission of any patient in the study but eventually showed CNS progression and was removed from study at month 11 for development of carcinomatous meningitis.

Patient R2 (Figure 2) had multiple posterior fossa lesions. Her MP dropped from 100% to 4% at month 2 with stability of lesion size volumetrically (14.3 to 13.7 cm<sup>3</sup>; 4% volume reduction). She died unexpectedly of unknown cause and no autopsy was performed. No evidence of tumor progression was found at her last staging study. No further information was available.

Patient R3 (Figure 3) had multiple tumors in the posterior fossa. Her MP dropped from 62% to 18% at month 2 but with concomitant enlargement of her tumor burden volumetrically (30% and from 3.7 to 4.8 cm<sup>3</sup>). RECIST criteria (13) could not detect this volume change and she remained on study as per clinical protocol. However, her tumors thereafter stopped growing and remained stable in volume through month 6, at which time she was removed from study because of late recognition by RECIST criteria (13) that her tumors had grown from baseline. All tumors were stable volumetrically during months 2–6, however. It is unknown how much longer her tumor volume might have remained stable on treatment.

For the two patients exhibiting a decrease in MP at month 2 and for whom longer-term data were available, progression free survival by clinical criteria was 8.5 + 3.5 months as compared to 3.9 + 1.6 months for the 19 patients without normalization of vessel shape.

### Normalization of vessel shape

By definition, a drop in an initially elevated MP indicates normalization of vessel tortuosity abnormalities. This normalization occurred both because of loss of small tortuous vessels and because of discernible “straightening” of larger arteries. Change in vessel radius also occurred during treatment for all four of the major named vessels analyzed. The radii of the paired frontopolar arteries were asymmetric at baseline (0.41mm for the highly tortuous left frontopolar artery and 0.66mm for the right) but became more symmetric at month 2 (0.42mm left and 0.45mm right). The radii of the posterior cerebral and superior cerebellar arteries both decreased (0.88 to 0.64 and 0.64 to 0.60 cm).

## DISCUSSION

This report describes quantitative changes to vessel shape visualized by MRA during treatment of brain metastases. Although MRA’s resolution precludes examination of capillaries, a striking finding was the widespread distribution of tortuosity abnormalities on baseline scan. Our methods averaged vessel shape parameters over the entire brain. Although this analysis must have included uninvolved vessels, average vessel tortuosity values were abnormal for every tumor patient at baseline. When we visualized the vasculature, we found that tortuosity abnormalities could extend to even major named vessels lying outside of apparent tumor confines. It is unknown whether these widespread abnormalities were related to the presence of disease indiscernible by gadolinium-enhanced imaging or to a general disorder of the intracerebral vasculature.

There was no apparent association between initial MP and subsequent reduction in MP. Tumor patients at baseline tended to possess a smaller vessel number and a lower average radius than healthy controls. Although this finding may appear paradoxical since cancer induces angiogenesis, two explanations are vessel dropout as a result of previous treatment or a reduction in imaged vessels because of increased intracranial pressure or local pressure effects. Tumor patients exhibiting improvement in MP at month 2 tended to exhibit an increase in vessel number at the second time point; one possible explanation is reduction of mass effect. The variables controlling the number of vessels seen by MRA are complex, and previous studies have concluded that tortuosity is more important than vessel number when assessing tumor-associated vasculature as seen by MRA (7,17).

One advantage of MRA as compared to traditional perfusion and permeability imaging is that individual vessels can be followed over time. Our study illustrates that vessel normalization includes not only reduction of vessel tortuosity but also alteration of vessel radii, with reduction of radii in some vessels and possible increases in others. Previous reports have described both increases and decreases in blood volume following tumor therapy (18,19). Our methods cannot assess permeability, but both permeability and tortuosity abnormalities might result from



cancer-induced alterations to the vessels wall. One report suggests that perfusion and macroscopic vessel analysis provide independent information (20). New research is needed that correlates vascular information at the “macroscopic” (MRA) and “microscopic” (blood volume, permeability) levels during longitudinal studies of tumor treatment.

An unanswered question is the effect of different therapeutic agents upon tumor vasculature. Most studies addressing vessel normalization employ agents that oppose vascular endothelial growth factor (VEGF). However, it seems reasonable to assume that any successful agent will exert some effect upon tumor vasculature. The drug examined here, lapatinib, is a dual inhibitor of the epidermal growth factor receptor (EGFR) and of ErbB-2 (Her2/neu) tyrosine kinase. The primary known effects are upon cell proliferation, but since both EGFR and HER2 may regulate VEGF expression and since tyrosine kinase may promote angiogenesis it is possible that lapatinib could have exerted some vascular effect.

Yet another unknown is the time course for vessel normalization as perceived by MRA. In our study, vascular normalization occurred in three patients after two months of chemotherapy. Vessel normalization may have occurred much earlier. If so, vessel morphological analysis might allow separation of responders from nonresponders earlier during treatment.

One limitation of our study was that too few patients responded to therapy to permit drawing definite conclusions about the value of using vessel tortuosity measurements in assessing treatment response. A second limitation was that too few imaging time points were available to determine the time course of vessel normalization. A third limitation is that controls were not age and sex-matched to tumor patients.

Nevertheless, this study demonstrates the feasibility of using noninvasive MRA to follow changes in vessel shape during tumor treatment. The initial results for prediction of therapeutic response appear promising.

## Acknowledgements

**Grants:** Various portions of this work were supported by: R01EB000219(NIBIB), P50CA89393-AV-55P(Avon), P50CA58185-AV-55P2(Avon), P30CA16086-29S1(NCI), P50CA089393-05S1(NCI), P30CA58223 (NCI), M01RR00046 (NIH), and ASCO YIA

## References

1. Folkman J. Tumor angiogenesis: therapeutic implications. *New England Journal of Medicine* 1971;285:1182–1186. [PubMed: 4938153]
2. Leach MO, Brindle KM, Evelhoch JL, et al. Workshop report: The assessment of antiangiogenic and antivascular therapies in early-stage clinical trials using magnetic resonance imaging: issues and recommendations. *British Journal of Cancer* 2005;92:1599–1610. [PubMed: 15870830]
3. Li CH, Shan S, Huang Q, Braun R, Lanzen J, Hu K, Lin P, Dewhirst M. Initial stages of tumor cell-induced angiogenesis: evaluation via skin window chambers in rodent models. *J Natl Cancer Inst* 2000;92:143–147. [PubMed: 10639516]
4. Baish JS, Jain RK. Fractals and cancer. *Cancer Research* 2000;60:3683–3688. [PubMed: 10919633]
5. Burger, PC.; Scheithauer, BW.; Vogel, FS. *Surgical Pathology of the Nervous System and its Coverings*. 3. Churchill Livingstone; New York: 1991.
6. Lenander C, Holmgren L. A novel method of visualizing vessels in human tumor biopsies. *Angiogenesis* 1999;291–293. [PubMed: 14517408]
7. Bullitt E, Zeng D, Gerig G, Aylward S, Joshi S, Smith JK, Lin W, Ewend MG. Vessel tortuosity and brain tumor malignancy: A blinded study. *Academic Radiology* 2005;12:1232–1240. [PubMed: 16179200]

8. McDonald MD, Baluk P. Significance of blood vessel leakiness in cancer. *Cancer Research* 2002;62:5381–5385. [PubMed: 12235011]
9. Jain RK. Normalization of the tumor vasculature: An emerging concept in anti-angiogenic therapy. *Science* 2005;307:58–62. [PubMed: 15637262]
10. Jain RK. Normalizing tumor vasculature with anti-angiogenic therapy: a new paradigm for combination therapy. *Nature Medicine* 2001;7:987–98.
11. Lin NU, Carey LA, Liu MC, Younger J, Come SE, Bullitt E, van den Abbeele A, Gelman R, Hochberg F, Winer EP. Phase 2 Trial of Lapatinib for Brain Metastases in Patients with HER2+ Breast Cancer. *ASCO*. 2006
12. Bullitt E, Lin N, Ewend M, Zeng D, Winer E, Carey L, Smith JK. Tumor Therapeutic Response and Vessel Tortuosity: Preliminary Report in Metastatic Breast Cancer. *MICCAI 2006; Lecture Notes in Computer Science* 2006;4191:561–568.
13. Therasse P, Arbuck SG, Eisenhauer EA, et al. New guidelines to evaluate the response to treatment in solid tumors: European Organization for Research and Treatment of Cancer, National Cancer Institute of the United States, National Cancer Institute of Canada. *J Natl Cancer Inst* 2000;92:205–216. [PubMed: 10655437]
14. Aylward SR, Bullitt E. Initialization, noise, singularities and scale in height ridge traversal for tubular object centerline extraction. *IEEE-TMI* 2002;21:61–75.
15. Bullitt E, Aylward S, Smith K, Mukherji S, Jiroutek M, Muller K. Symbolic Description of Intracerebral Vessels Segmented from MRA and Evaluation by Comparison with X-Ray Angiograms. *Medical Image Analysis* 2001;5:157–169. [PubMed: 11516709]
16. Bullitt E, Gerig G, Pizer SM, Lin W, Aylward SR. Measuring tortuosity of the intracerebral vasculature from MRA images. *IEEE-TMI* 2003;22:1163–1171.
17. Bullitt E, Wolthusen A, Brubaker L, Lin W, Zeng D, Van Dyke T. Malignancy-associated vessel tortuosity: A computer-assisted, MRA study of choroid plexus carcinoma in genetically engineered mice. *AJNR* 2006;27:612–619. [PubMed: 16552004]
18. Wildiers H, Guetens G, De Boeck G, Verbeken E, Landuyt B, Landuyt W, de Bruijn EA, van Oosterom AT. Effect of antivascular endothelial growth factor treatment on the intratumoral uptake of CPT-11. *J Pancreas* 2006;7:163–173.
19. Willett CG, Boucher Y, di Tomaso E, Duda DG, Munn LL, Tong RT, Chung DC, Sahani DV, Kalva SP, Kozin SV, Mino M, Cohen KS, Scadden DT, Hartford AC, Fischman AJ, Clark JW, Ryan DP, Zhu AX, Blaszkowsky LS, Chen HX, Shellito PC, Lauwers GY, Jain RK. Direct evidence that the VEGF-specific antibody bevacizumab has antivascular effects in human rectal cancer. *Nat Med* 2004;10:145–147. [PubMed: 14745444]
20. Parikh A, Smith JK, Ewend MG, Bullitt E. Correlation of MR perfusion imaging and vessel tortuosity parameters in assessment of intracranial neoplasms. *Technology in Cancer Research and Treatment* 2004;3:585–590. [PubMed: 15560716]



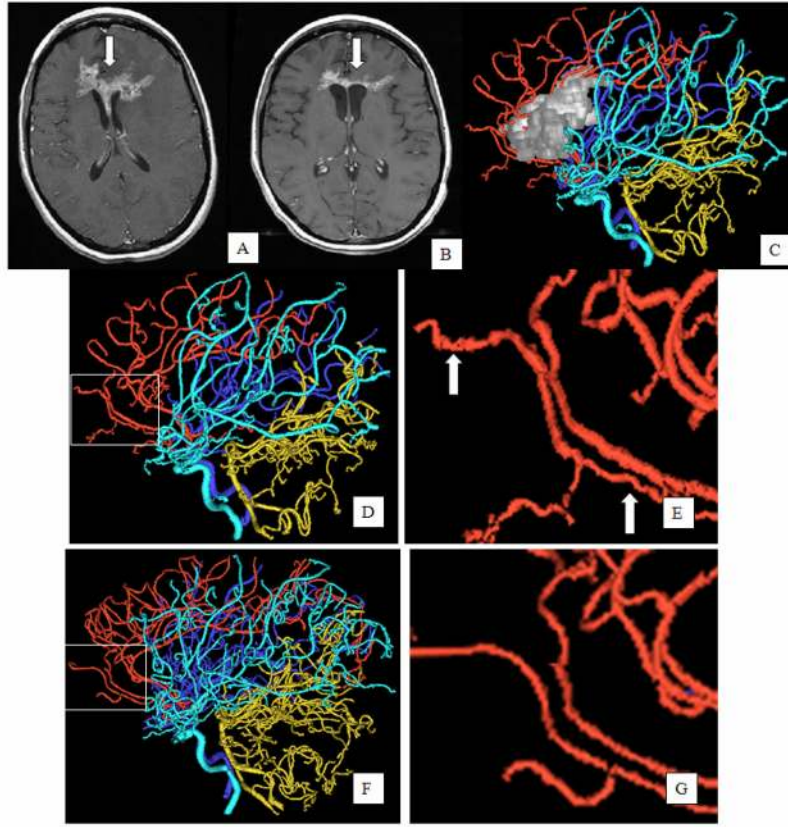


**Figure 1.** Normalization of vessel shape during treatment. **A:** Axial, gadolinium-enhanced, T1-weighted MR slice (mp-rage, TR/TE 1700/4.38, inplane resolution  $0.9 \times 0.9$  mm, interslice spacing 3 mm) through the center of the tumor (arrow) at baseline. **B:** Similar slice obtained using the same parameter settings at month 2. Note reduction in tumor size. **C:** 3D rendering of the intracerebral vessels and of the patient's segmented tumor (grey) from a lateral point of view (nose to left) at baseline. The vessels are color-coded by circulatory group. **D:** Similar rendering of vessels at baseline but with the tumor visualization turned "off". The white rectangle indicates the region magnified in E. Note that this region extends outside tumor margins. **E:** Magnified region of the frontopolar arteries at baseline. Arrows point to the markedly abnormally tortuous left frontopolar artery. The right frontopolar artery courses parallel to and just above the left frontopolar from this point of view; note that it appears dilated. Multiple medium sized and small vessel branches in the vicinity are abnormally tortuous. **F:** 3D rendering of the intracerebral vessels at month 2 from the same point of view as C-E. The white rectangle depicts the region magnified in G. **G:** Magnification of the region of the frontopolar arteries at month 2. As compared to the magnification of the baseline vessels shown in E, note the "straightening" of the left frontopolar artery, the reduction in radius of the right frontopolar artery, the "straightening" of medium sized branches, and the loss of small, abnormal vessels.

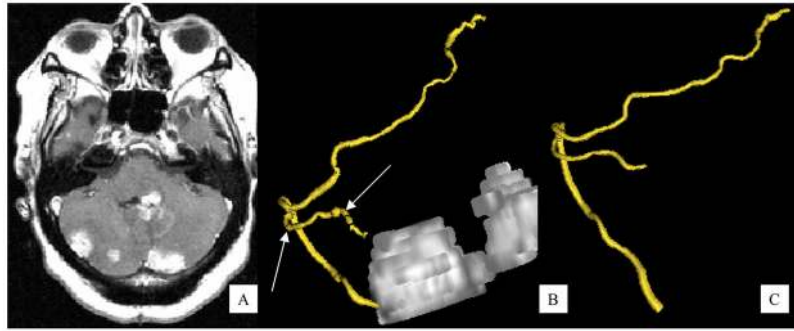


**Figure 2.** Normalization of vessel shape during treatment. **A:** Axial, gadolinium- enhanced, T1-weighted MR image (mp-rage, TR/TE 1700/4.38) at baseline. There are multiple cerebellar tumors. **B:** 3D rendering of the segmented tumors (grey) and of the basilar, left superior cerebellar, and left posterior cerebral arteries at baseline as shown from a lateral point of view. Note the abnormal tortuosity of the left superior cerebellar artery (arrows). The posterior cerebral artery is also abnormal, although to a lesser degree. **C:** Rendering of the same vessels from the same point of view at month 2. Note the arterial “straightening”.

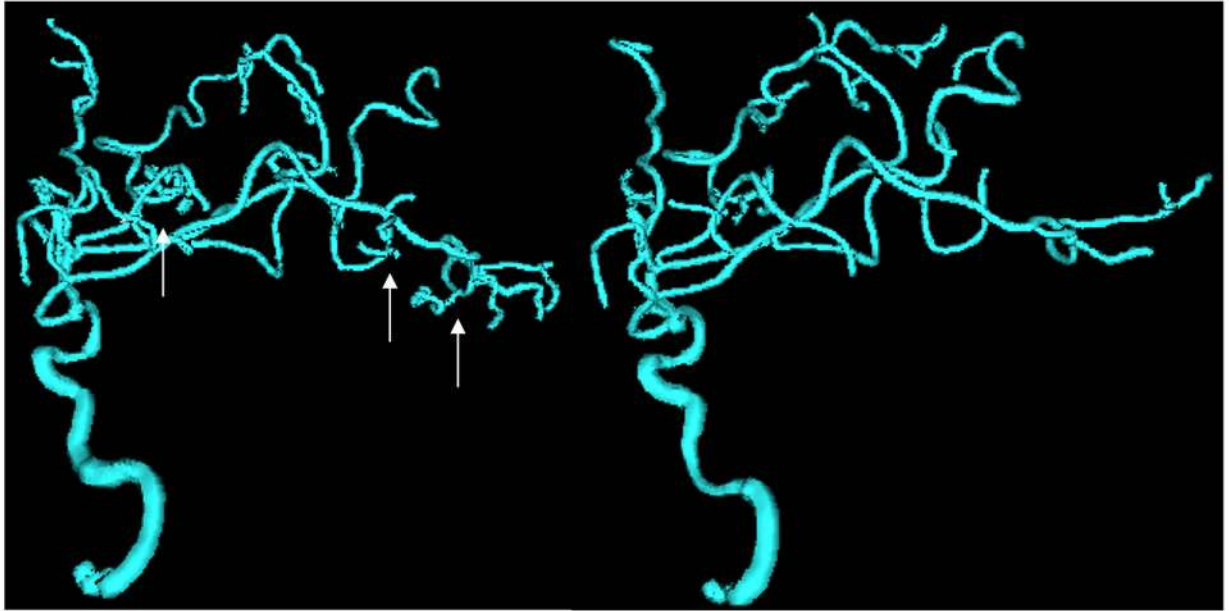


**Figure 3.** Loss of small abnormal vessels during treatment. **A:** Left middle cerebral circulation shown at baseline and rendered from a lateral point of view. Arrows point to clusters of small, abnormal vessels that are not visualized at month 2. **B:** Similar rendering at month 2.

Table 1

Means and standard deviations of vessel number (VN), average radius (RAD), tortuosity as measured by SOAM (SOAM), tortuosity as measured by ICM (ICM), and Malignancy Probability (MP) for 34 healthy volunteers and for 22 breast cancer patients at baseline and at month 2. Results for cancer patients are presented for the group as a whole, for those without subsequent improvement in MP (19 cases), and for those with subsequent reduction in MP (3 patients). N/A = non-applicable (healthy tortuosity data are used to normalize tortuosity values during calculation of the MP for tumor patients and so MP is not applicable to the healthy group). Note that there is no apparent association between initial MP and subsequent reduction in MP, that tumor patient baseline vessel numbers tend to be lower than those of healthy controls, and that tumor patients exhibiting improvement in MP at month 2 tend to show an increase in vessel number at the second time point.

	Vessel Shape Measures				
	VN	RAD	SOAM	ICM	MP
Healthy	255.2 + 53.3	0.59 + 0.03	3.36 + 0.21	4.12 + 0.73	N/A
Baseline	204.0 + 65.8	0.56 + 0.08	4.31 + 0.65	4.88 + 1.24	88.4 + 22.8
Month 2	205.5 + 74.4	0.56 + 0.07	4.02 + 0.41	4.80 + 1.03	81.6 + 27.8
Baseline	210.8 + 67.5	0.54 + 0.07	4.32 + 0.68	4.83 + 1.00	88.6 + 22.8
Month 2	203.3 + 65.6	0.55 + 0.07	4.13 + 0.32	4.81 + 1.09	88.6 + 22.2
Baseline	160.3 + 33.8	0.65 + 0.08	4.26 + 0.49	5.19 + 2.62	87.3 + 21.9
Month 2	219.3 + 138.0	0.58 + 0.10	3.34 + 0.30	4.77 + 0.63	40.0 + 23.1